



Research paper

Analysis of deformations of road embankments founded on displacement columns improving soft subsoil

Waldemar Szajna¹, Liudmyla Bondareva², Bartosz Szatanik³

Abstract: Drilled displacement columns, constructed in the form of unreinforced or reinforced concrete elements, are currently a very commonly used method of improving soft subsoil, creating an alternative to more expensive pile foundations. A frequently used solution for improving soft soils of road or railway embankments is to design a regular pattern of columns of relatively small diameter. Columns along the perimeter of the improved area are reinforced with rigid steel profiles, while the internal ones are made as concrete elements. Column heads are usually covered with a load transfer platform (layer of compacted granular fill) which is additionally reinforced with geosynthetics.

The application of soil improvement with displacement columns is not always successful. It is due to the errors and shortcomings occurring at the design stage, including simplifications in modelling, to construction faults, which may include insufficient experience of contractors and/or improper supervision.

Referring to the real object that failed, the article provides the results of numerical parametric analyses taking into account the influence of the key design parameters such as: the stiffness of the load transfer layers, the amount and stiffness of the geosynthetic reinforcement as well as the column spacing. The article presents comparisons of numerical results obtained with the finite element analyses for various approaches to geometry modelling (axisymmetric, 2D and 3D). The simulations indicate that the use of the axisymmetric model of a single column in routine design may lead to the deformations exceeding the serviceability limit states.

Keywords: drilled displacement columns, FEM parametric study, road embankments, soil improvement

¹DSc., PhD., Eng., University of Zielona Góra, Institute of Civil Engineering, Prof. Zygmunta Szafrana 1 Street, 65-516 Zielona Góra, Poland and TPA – Technical Research Institute, Parzniewska 8 Street, 05-800 Pruszków, Poland, e-mail: W.Szajna@ib.uz.zgora.pl, ORCID: 0000-0001-6230-768X

²PhD., Eng., Kyiv National University of Construction and Architecture, 31 Povitroflotskiy avenue, 03037, Kyiv, Ukraine and TPA – Technical Research Institute, Parzniewska 8 Street, 05-800 Pruszków, Poland, e-mail: skochko.lo@knuba.edu.ua, ORCID: 0000-0001-7392-814X

³MSc., Eng., TPA – Technical Research Institute, Parzniewska 8 Street, 05-800 Pruszków, Poland and MSc., Eng., TPA – Technical Research Institute, Parzniewska 8 Street, 05-800 Pruszków, Poland, e-mail: bartosz.szatanik@tpaqi.com, ORCID: 0009-0009-8292-5704

1. Introduction

Soil improvement has become an important element of transport infrastructure engineering. More than 75% of soil improvement projects are concerned with development of transportation infrastructure [1]. There is a vast range of available soil improvement methods [2, 3].

Many communication routes cross the areas of loose or unconsolidated surface layers of Holocene deposits, often containing deformable organic material. The use of soil improvements in the form of various types of columns [4] which transfer loads to deeper, load-bearing soil layers, is common in such situations. One of the technology used particularly frequently, are Drilled Displacement Columns (DDCs) which provide the foundation of road or railway embankments.

DDCs are implemented in the form of concrete elements, usually with a diameter of 30–40 cm. The columns around the perimeter of the improved area are usually reinforced with steel I profiles. In the general classification of soil improvements, they are regarded as rigid inclusions. The arrangement of columns for embankments, covered with a load transfer platform (LTP) of compacted granular fill, with additional geosynthetic reinforcement is referred to as Geosynthetic-reinforced column-supported embankments (GRCSEs). The work by Simon et al. [5] presents a detailed characteristic of the technology. Such solutions provide an alternative to more expensive foundation piles. Significant differences between the technologies of columns and piles are discussed in [6].

The widespread use of DDCs results from their numerous advantages [7, 8]. Among the technical advantages, the increase in soil compaction in the vicinity of the column should be mentioned [9]. Structure achieves settlement reduction. The other include no excavated material, no noise and vibrations, additionally DDC is characterized by high installation speed and competitive costs.

The main disadvantages of the technology are: possible ground heave and horizontal displacements of the adjacent columns. DDCs should not be used in soils with undrained strength $c_u < 15$ kPa (hydrostatic concrete pressure must be lower than soil strength).

The GRCSE technology is characterized by a complex load transfer mechanism [10]. The authors identified three phenomena occurring in this mechanisms: A) soil arching, B) tensioned membrane effect, and C) stress concentration due to column-soil stiffness differences. If the GRCSE is properly designed and constructed an arching effect occurs in its transmission layer [11], thanks to which the main part of the loads is transferred to the columns. The redistribution of the loads (generated by the embankment) from the soft soil to the columns is enhanced by the membrane forces arising in the geosynthetic reinforcement [12]. Despite the concentration of stresses at the heads of the columns, a layer of soft subsoil is subjected to some vertical loads, which cause downdrag force in the upper part of the shaft of the columns.

DDC technology has been the subject of many studies, using laboratory models [13–15] (including centrifuge [16]), field studies e.g. [17, 18] and numerical analysis e.g. with the Finite Element Method (FEM) [19, 20] and with the Discrete Element Method [21].

The impact of column installation methods on changes in soil conditions, displacements and on neighbouring columns is presented in [22, 23].

The risk of failure with respect to particular soil improvements methods is analysed in [24, 25]. Due to the ductile/brittle behaviour of the systems, the authors differentiate the technologies into three groups. They include the DDC technology into the group of increased risk of failure, characterized by brittle behaviour. In soft soil, concrete columns constitute relatively rigid elements. In the absence of reinforcement, small diameter DDCs are both brittle and vulnerable to fracture. The structure does not signal a pre-emergency state of stresses. The use of additional geosynthetic reinforcement increases the ductility of the system.

Despite the availability of numerous research results of GRCSEs, their failures still occur. The motivation for the presented research is the case of a road on a low embankment, made on a soft organic subsoil reinforced with columns, on which large differential settlements of the surface occurred.

The aim of the work is to examine the sensitivity of the system to changes in the values of essential design parameters, such as: geometry and stiffness of the LTP, the amount and stiffness of geosynthetic reinforcement and the spacing of columns, as well as its susceptibility to the method of spatial modelling of the structure geometry. The problem was solved in the form of parametric analyses using FEM. A comparison of the results obtained for axisymmetric models of single columns (common approach in Polish practice), 2D models in a plane strain state and 3D models is presented. When analysing the results, the focus was put on displacements.

2. Overview of the case study

A local road, constructed on a low column-supported embankment ($H \approx 1.7$ m) experienced excessive, uneven settlement soon after its commissioning. The embankment was constructed in the winter season. In the summer, when the asphalt pavement was being laid, some cracks of several millimetres appeared at the outer curbs of the sidewalks. Then, the cracks (accompanied with irregularities) formed within the sidewalk and the edges of the road surface, taking the characteristic “egg carton” shape with depressions beyond the zone of column heads. The cracks in the asphalt pavement also occurred in the cycle path on the opposite side of the road. Due to the above mentioned, in the selected 10 profiles, the settlements were measured between the heads of the columns, Fig. 1. In the first series of tests, they ranged from 5 to 17 mm. Five weeks later, the settlements increased and ranged from 5.5 to 23 mm, indicating large horizontal soil variability.



Fig. 1. The view of pavement settlements between column heads

On the several-hundred-meter distance, where the embankment was constructed, the area is covered with a layer of Holocene peat with a thickness of 5–6 m. Beneath the peat there is a layer

of medium sands, of variable thickness, covering the silts. A typical cross-section illustrating the ground conditions, together with the results of the CPTu and DMT tests superimposed on the calculation model, is shown in Fig. 2.

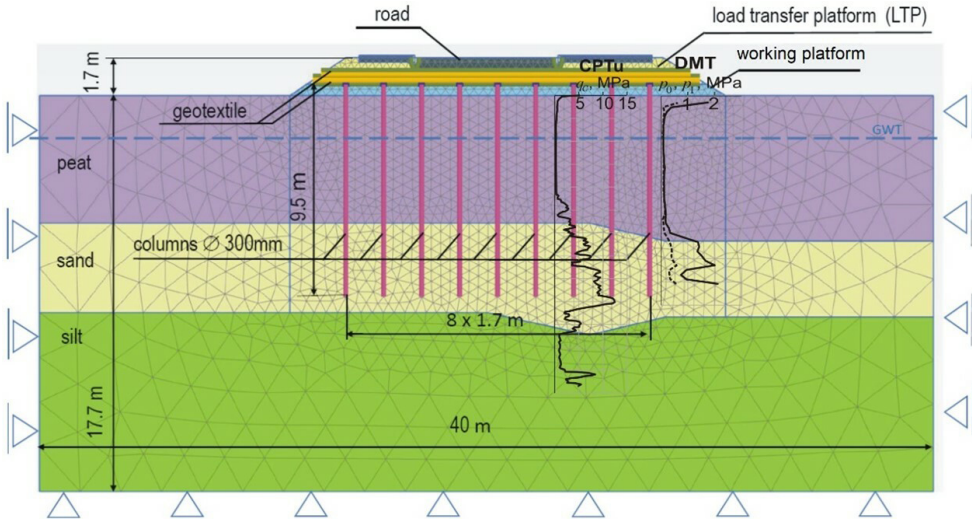


Fig. 2. Typical cross-section of the embankment structure with the geotechnical layers and superimposed results of CPTu and DMT tests

In the peat layer, the average cone resistance values q_c have been 0.2 MPa. The dilatometer tests have confirmed the low values of peat stiffness parameters. The layer of sands is in a medium-dense state, and in the case of silts, the average undrained shear strength $c_u \approx 40$ kPa. The groundwater table is at a depth of 2 m. The bases of the columns supporting the embankment are installed in the sand.

The construction of the embankment required preparation of a 0.5 m thick working platform, from which the displacement concrete columns (C16/20) of a diameter of $D_c = 0.3$ m were installed, without widening caps. Above the heads of the columns, a load transfer platform (0.5 m thick) was made of compacted granular fill, reinforced with two layers of polyester (PET) geotextile, with a minimum tensile strength of 150 kN/m.

The arrangement of the columns in the plan view is shown in Fig. 3a. The figure also shows the plan view of soil unit cell A_s per one column. This value makes it possible to determine the so-called Area Replacement Ratio ($ARR = (A_c/A_s)100\%$), where A_c is the cross-sectional area of the column. Figure 3b shows the equivalent arrangement of columns, which facilitates 2D analyses.

The completed embankment meets the minimum height condition specified in the BS 8006 standard as $H_{\min} > 0.7(L_{\max} - a)$, where L_{\max} is the maximum axial spacing of the columns, and a is the width of the cap of the column head. In the considered case (column heads without widening caps $a = D_c$) $H_{\min} > 0.98$ m. Due to the additional condition presented in the standard, $H = 1.7$ m $< 2H_{\min} = 1.96$ m, the embankment should be regarded as relatively low.

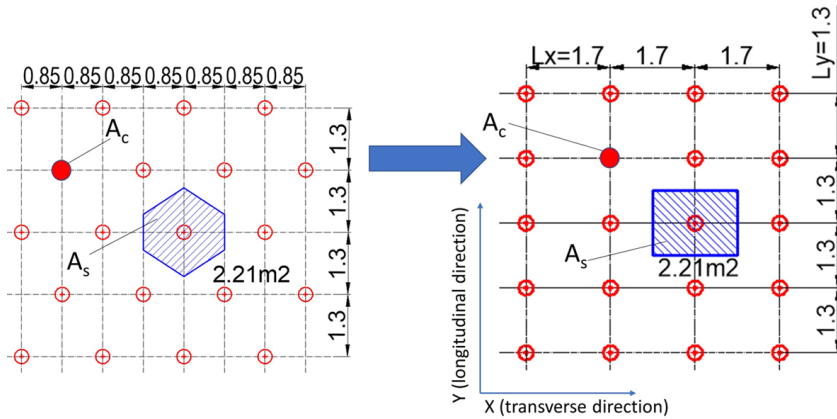


Fig. 3. Arrangement of columns: a) actual arrangement, b) equivalent arrangement

In such cases, the road structure is usually exposed to uneven “egg carton” settlement caused by the reduction of the soil arching effect. The analysed case belongs to this class of problems.

3. Description of numerical models

The load transfer mechanism in GRCSE facilities is complex. It includes the soil arching phenomenon, the transfer of tensile forces from the geosynthetic to the column heads and the redistribution of vertical stress component from the ground to the columns due to the difference in stiffness of these elements. In order to quantitatively compare the impact of basic design parameters on the values of displacements in the system, a number of FEM numerical analyses were performed. The parametric study concerned: column spacing, geosynthetic reinforcement characteristics and stiffness of the transmission layer. In subsequent simulations the spatial modelling of the entire system was changed from 3D through 2D to axial symmetry. The description of the data variants taken for analysis is presented in Table 1 (soil parameters will be presented further).

In each modelling method described, the dataset corresponding to the real object is called a basic one. In subsequent variants, one design parameter was arbitrarily overestimated and then underestimated in order to determine the object’s sensitivity to change. In total, calculations were made for 1t variants, divided into 5 groups, marked with Roman numerals.

Group I consists of 3 basic referential models. Variant AX-b refers to the modelling of a single column together with the adjacent soil, in conditions of axial symmetry. To ensure equivalence of the axisymmetric model with the real spatial spacing of columns L_x and L_y (Fig. 3b), the rectangular impact area of a single column was replaced with a circular area of the same cross-section.

Table 1. Variants of numerical analysis

Group of features	Description	Model symbol	Column spacing [m × m]	ARR [%]	Geotextile		LTP stiffness
					No. of layers	EA [kN/m]	E_{ref} [MPa]
I Basic models	basic axisymmetric model	AX-b	1.7 × 1.3	3.20	2	1250	40
	basic 2D model	2D-b					
	basic 3D model	3D-b	1.7 × 1.3 triangular arrangement				
II Similar to AX-b, different column spacing, axisymmetric models	spacing 1.4 × 1.4	AX-1	1.4 × 1.4	3.61	2	1250	40
	spacing 1.7 × 1.5	AX-2	1.7 × 1.5	2.77			
	spacing 1.7 × 1.7	AX-3	1.7 × 1.7	2.45			
	spacing 1.7 × 1.3 without geotextile	AX-4g	1.7 × 1.3	3.20	–		
III Similar to 2D-b, different column spacing, plain strain models	spacing 1.7 × 1.7	2D-s1	1.7 × 1.7	2.45	2	1250	40
	spacing 1.7 × 1.5	2D-s2	1.7 × 1.5	2.77			
	spacing 1.4 × 1.4	2D-s3	1.4 × 1.4	3.61			
	spacing 1.3 × 1.3	2D-s4	1.3 × 1.3	4.18			
IV Similar to 2D-b, different geotextiles, plain strain models	lower geotextile 1 × PET150	2D-g1	1.7 × 1.3	3.20	1 (lower)	1250	40
	upper geotextile 1 × PET150	2D-g2	1.7 × 1.3		1 (upper)	1250	

Continued on next page

Table 1 – Continued from previous page

Group of features	Description	Model symbol	Column spacing [m × m]	ARR [%]	Geotextile		LTP stiffness
					No. of layers	EA [kN/m]	E_{ref} [MPa]
IV Similar to 2D-b, different geotextiles, plain strain models	without geotextile	2D-g3	1.7 × 1.3	3.20	–	–	
	basic geotextile 2× PET300	2D-g4	1.7 × 1.3		2	3000	
V different LTP stiffness	20 MPa	2D-e1	1.7 × 1.3	3.20	2	1250	20
	60 MPa	2D-e2	1.7 × 1.3				60

Axisymmetric (AX); Plane strain (2D); Full 3D space (3D)

The basic variant 2D-b refers to GRCSE modelling for the plane strain conditions. The basic variant 3D-b is a full spatial simulation of a real structure.

In group II, which concerns modelling of a single (central) column in the axisymmetric condition, 4 additional variants (AX-1 to AX-4) were considered, taking into account different spacings.

The next group (numbered III) consists of 4 variants of data for which calculations were performed for a plane strain state, assuming various column spacings. Other parameters of the system were adopted as in the basic model. The variants are marked with the symbols 2D-s1 to 2D-s4.

The next two groups of variants (IV ÷ V) also refer to the plain strain model. In group IV, the parameters of geosynthetic reinforcement were changed. Four variants (2D-g1 ÷ 2D-g4) were considered, in which the amount of reinforcement was varied, the tensile stiffness of the reinforcement EA (E – Young's modulus A – reinforcement cross-sectional area), in turns the upper or the lower layer or both geotextile layers were excluded.

In group V, which concerns the Load Transfer Platform (LTP), Young's modulus was altered (variants 2D-e1 and 2D-e2).

An illustrative parameter characterizing each variant is the ARR .

3D models realistically reflect the geometry of the GRCSE and the interaction of the columns with the surrounding soil, but both the time to prepare the model and the time for spatial analysis is a considerable limitation. The 2D plane strain state models introduce restrictions to the simulation of column-soil interaction. This interaction is an eminently three-dimensional phenomenon. The columns are spaced pointwise at constant discrete distances in the out-of-plane direction. However, Plaxis 2D [26], through the embedded beam mechanism [27], enables modelling of columns while taking into account their spacing and real parameters of the columns, ensuring the mutual interaction of soil on both sides of the columns. Axisymmetric models reflect only the behaviour of a column axially loaded, located in the centre of an infinitely large improved area. Despite this shortcomings, this method is commonly used in design practice.

Constitutive models and parameters of individual soil layers are presented in Table 2. Each natural soil layer was treated as normally consolidated. The Hardening Soil Model (HSM) was adopted for the natural soils. The working platform and the load transfer platform have been simulated with the Coulomb–Mohr (MC) model. Most of the parameters have been adopted as in the engineering design, the others have been determined by interpreting the results of CPTu [28] and DMT [29].

The measured values of pavement settlements in the fields between adjacent columns differ up to three times and prove the high horizontal variability of the subsoil characteristics. This variability, with limited information about the subsoil, makes it impossible to calibrate numerical models that allow for quantitative compliance of calculation results with measurements.

As far as a numerical analysis type is concerned, in each AX, 2D and 3D models, the consolidation, drained analyses were applied, with time intervals corresponding to real time phases of the road construction. In 2D and 3D cases, columns were modelled as “embedded beams”. These types of elements do not allow introduction of an interface element between columns and soil. However, the interface elements were used between soil and geosynthetic layers.

Table 2. Soil parameters

Soil type	Soil model	γ [kN/m ³]	c' [kPa]	ϕ' [°]	ψ [°]	E [MPa]	$E_{\text{oed ref}}$ [MPa]	$E_{50 \text{ ref}}$ [MPa]	$E_{\text{ur ref}}$ [MPa]	k_h [m/s]	k_v [m/s]
peat	HSM	10	7	8	0	–	0.4	0.4	1.2	1.16E-7	5.79 E-8
sand	HSM	20	0	34	4	–	90	90	270	0.00017	0.00017
silt	HSM	20	5	27	0	–	45	45	135	5.79E-8	5.79E-8
LTP	MC	21	2	33	3	40	–	–	–	1.16E-6	1.16E-6
working platform	MC	20	2	31	1	20	–	–	–	5.79E-5	5.79E-5

4. Results and discussion

First, let us analyse the results obtained for columns in the axisymmetric state. The influence of the spacing between the columns is reflected by the size of the R_x radius of the soil cell associated with the column. Figure 4 shows the diagram of a model obtained from the numerical simulations and the settlement curves of the columns. These are variants of models from group II supplemented with the basic model AX-b (Table 1). The courses of the curves are in line with the intuition but for one exception. In general, an increase in the spacing of columns or the ARR results in both the increase of settlements and settlement differences. The effect is particularly strong when a relatively small increase in ARR , from 3.2% to 3.61%, results in

very significant increases of differential settlements. The exception is the solution obtained for AX-4g model (without reinforcement) where practically no differential settlements is observed. The peculiar nature of the solution is probably the effect of boundary conditions, but the more detailed explanation needs additional research.

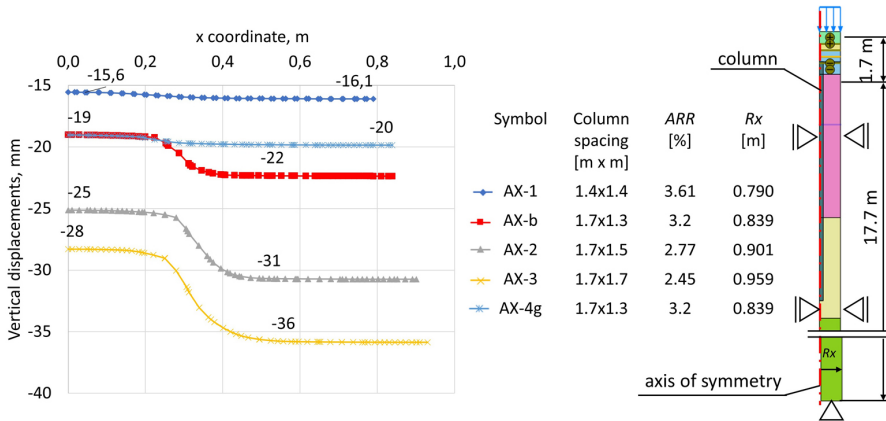


Fig. 4. Settlements obtained for the axisymmetric models and the view of the AX-b model

Subsequent analyses refer to the 2D models. Figure 5 shows the distribution of vertical displacement in the 2D-b basic model. A considerable settlement of the right edge of the embankment is visible. The settlement is caused by the layout of columns in this sector and the increase in peat depth. The inserted graph shows settlement values in millimetres.

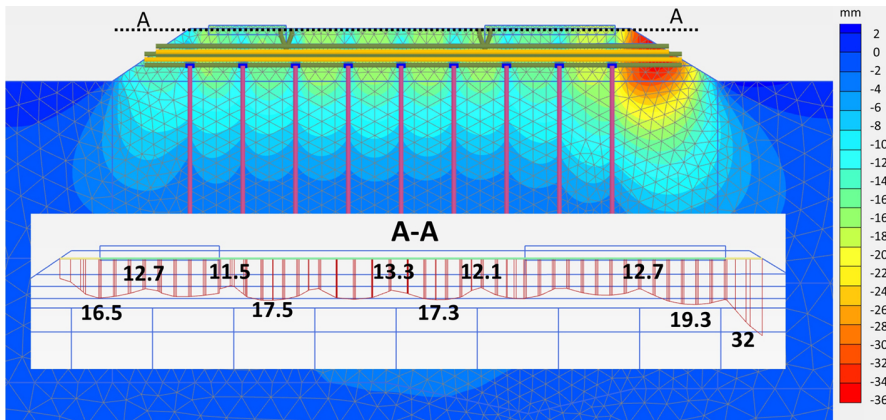


Fig. 5. Distribution of vertical displacements in the 2D-b basic model

Figure 6 shows a comparison of the results of settlement for variants of group III models (Table 1) in which the spacing of columns was the variable. The figure shows that the increase in the spacing of the columns in relation to the basic one ($ARR = 3.2\%$) obviously increases the differential settlements and the settlement of the column heads.

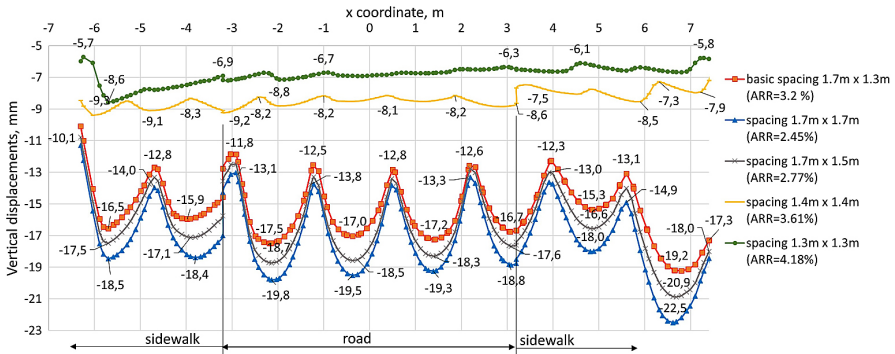


Fig. 6. Impact of column spacing on settlements (variants 2D-s1 ÷ 2D-s5 & 2D-b)

The qualitative difference in the results is visible when the reinforcement percentage increases slightly to the value of $ARR = 3.61\%$. This change significantly reduces differential settlements and significantly reduces the average settlement in the entire cross-section (the reduction of settlements of the right edge of the embankment is concerned with a new layout of columns). The above effects are even more pronounced when $ARR = 4.18\%$. The comparisons suggest that there is a limit value of the column spacing below which, at a low cost, it is possible to significantly reduce the deformation of the system.

The purpose of the next 2D analysis was to compare the effects that can be achieved by changing the parameters of the geosynthetic reinforcement layer. The results are shown in Fig. 7a. The figure shows that even doubling the amount of reinforcement compared to the basic solution reduces the average settlements and settlement differences in a very moderate way. On the other hand, the exclusion of one layer of reinforcement in the basic solution increases the settlements slightly. However, the lower layer of reinforcement is of greater importance in reducing displacements.

Interesting results are obtained in the solution where the geosynthetic reinforcement is excluded from the system. According to intuition, the edges of the embankment settled strongly in the absence of constraints that would be provided by reinforcement. Because of this horizontal spread of the embankment, the values of the differences in settlement were reduced significantly.

In order to make it easier to compare the values of the differences of settlement in the particular variants, these differences are shown in the lower part of Fig. 7b. Its upper part presents the secant lines connecting the points on the surface located above the column heads. These secants represent the measuring beam in Fig. 1. In relation to them, the settlement differences visible in the lower part of the graph were calculated.

The influence of the stiffness of LTP on the size of settlement is shown in Fig. 8. The analysis includes both insufficient and very good aggregate compaction of this layer. Its results indicate that when the basic value of the Young's modulus (40 MPa) is reduced by 50%, the value of the settlement increases slightly. On the other hand, the increase in the basic value of the modulus by 50% reduces the settlement and the settlement differences only insignificantly. However, these are not qualitative differences, as shown by the increase in ARR from 3.2 to 3.61% in Fig. 6.

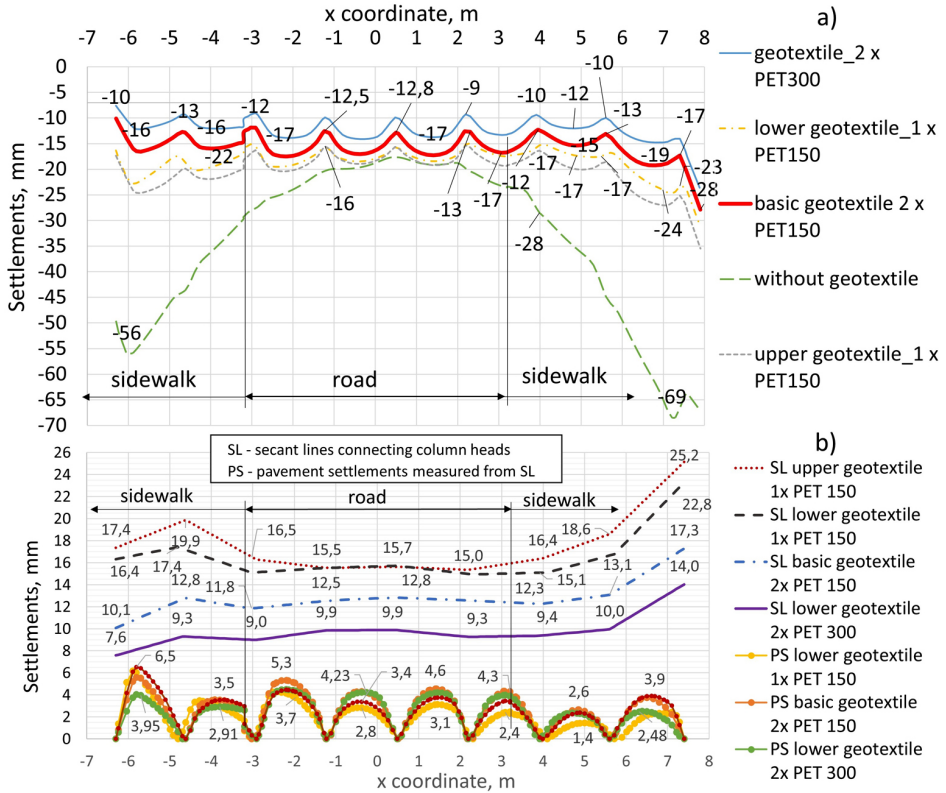


Fig. 7. Influence of geotextile on settlements: a) total settlements, b) secant lines connecting column heads and pavement settlements measured from secant lines (variants 2D-g1÷2D-g5 & 2D-b)

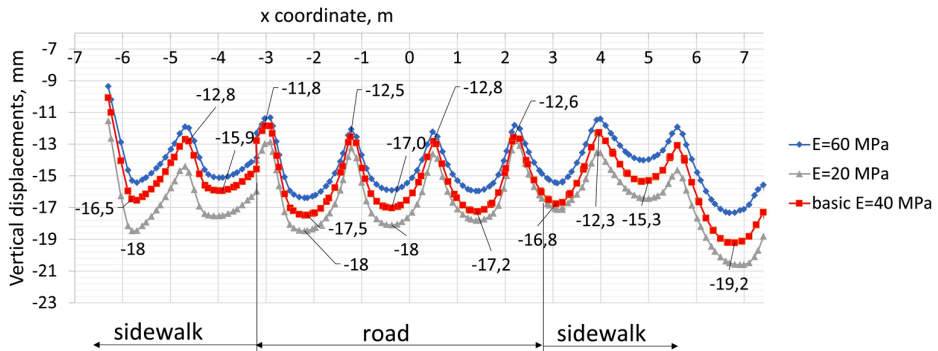


Fig. 8. Influence of LTP stiffness on settlements

Considering the 3D modelling, Fig. 9a shows a general diagram of the problem. Despite a slight lack of symmetry resulting from the arrangement of layers (Fig. 2), it was decided to analyse only half of the width of the embankment, assuming that the task is symmetrical.

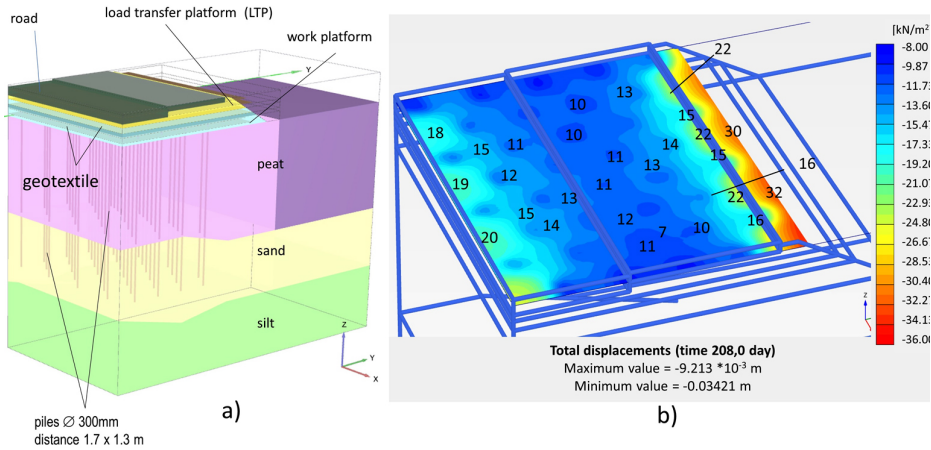


Fig. 9. 3D basic model: a) model elements, b) total displacements in the embankment surface

Figure 9b presents surface settlement, taking a characteristic “egg carton” shape. In order to improve readability of the figure, numbers depicting settlement values were superimposed on the contour lines. The values are slightly lower than those recorded in the second series of referential measurements and correspond to the values from the first series. This means that the stiffness parameters of the numerical model are overestimated in relation to the real ones. Nevertheless, a comparative analysis of the particular 3D, 2D and axisymmetric numerical results is possible.

Figure 10 shows the superimposed displacement graphs obtained for all basic models AX-b, 2D-b and 3D-b. The graphs show that the highest settlement values were obtained for the single column model in the conditions of axial symmetry. They are almost twice as large as for the settlement of the 3D-b model in the central zone. Also, the differences in settlement between the head and the inter-column zone exceed the values for the 3D-b model. Nevertheless, the AX-b model does not reflect the significant problem of the adopted design solution, i.e. the slide of the embankment edge in the horizontal direction.

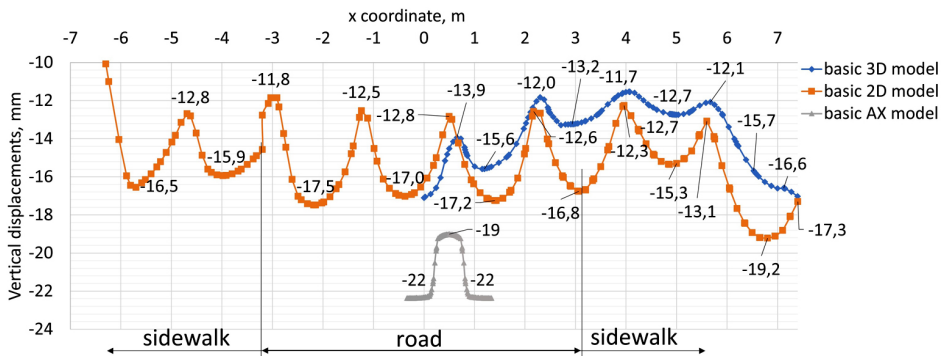


Fig. 10. Settlements of three basic models: axisymmetric, 2D and 3D

The results of the average settlement obtained in the 2D-b solution (plane strain state) are more similar to the results from the 3D model. This model also correctly reflects the problem of the right edge of the embankment. However, the differences in settlement over the head and in the inter-column zone are significantly overestimated here.

The obtained differences between the axisymmetric and the 3D models are much greater than those described in [30]. The differences obtained there almost disappeared when the authors changed the boundary conditions in the model base by introducing additional horizontal constraints. In the present study, despite the fact that such bonds were present in each analysis (Fig. 2), the differences were significant.

In order to examine the differences, as suggested in [11], it is reasonable to analyse the arching effect. Figure 11 shows the principal stress trajectories obtained for the basic model (column spacing 1.7×1.3 m; $ARR = 3.2\%$) and the 2D-s4 model (column spacing 1.3×1.3 m; $ARR = 4.18\%$). In the 2D-s4 model, thanks to the small spacing of the columns, the arching could develop in a greater degree. However, in the basic model (Fig. 11a), the flattened system of the trajectories in the upper zone of the inter-column space indicates that full arching has not developed here. It seems that this phenomenon may be the main reason for the differences in displacements obtained in the solutions.

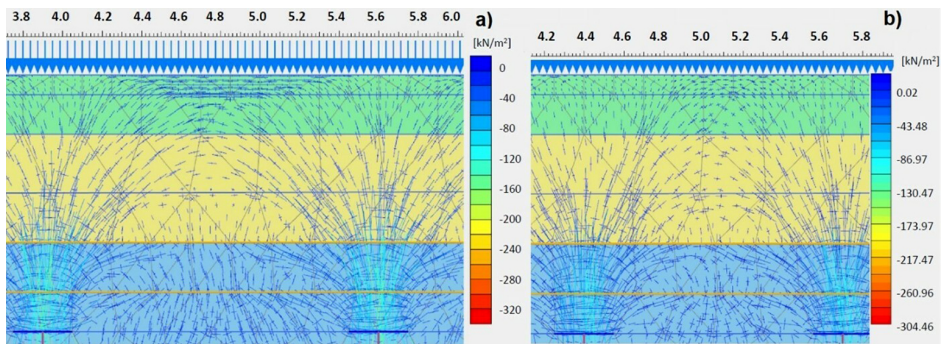


Fig. 11. Trajectories of principal stresses in the following models: a) basic 2D-b, b) 2D-s4

A significant problem for low embankments is related to the formation of settlement between the columns. The distribution of stresses between the column heads and the soft soil plays a key role here, which is due to the arching phenomenon. The more stress is transferred to the head, the less settlement occurs between the columns. The value of the force transferred by the column head, related to the force transferred by the area per one column, is called load transfer efficiency

$$(4.1) \quad E_f = \frac{\sigma_{cm} A_c}{\sigma_{sm} A_s} 100\%$$

where: σ_{cm} and σ_{sm} are, respectively, the average stress on the head of the column and the soil between the columns, A_c and A_s are the column and the soil cross-sectional areas, respectively (Fig. 3b).

In order to determine the relationship between the load transfer efficiency and the maximum settlement of the adjacent soil zone, for each version of the model described in Table 1, these values have been determined. In the case of 2D and 3D models, the calculations were performed only for the central columns, because, as previously indicated, the models of axial symmetry simulate the behaviour of centrally located columns in the area of soil improvement. The results are shown in Fig. 12. The red markers refer to the solutions for basic models.

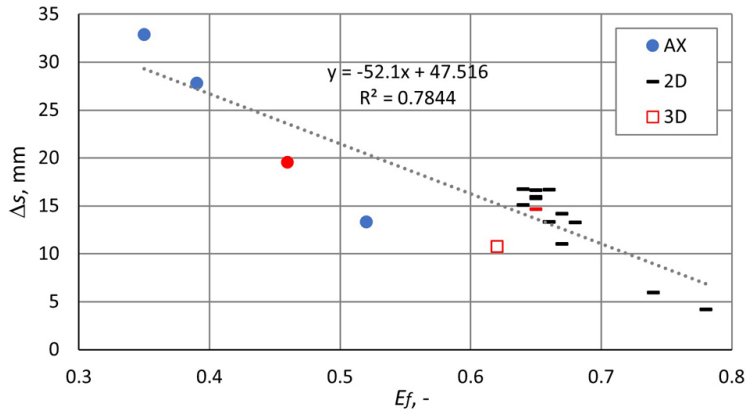


Fig. 12. Relationship between the efficiency and the difference in settlement of the inter-column zone

Figure 12 shows that the efficiency of columns modelled as axisymmetric is the lowest, which translates into large differences in settlement. The result obtained for the central column in the 3D model is surprising. Although the efficiency of this column is lower than that of the central column in the 2D model, the settlement differences are also lower. In order to explain the phenomenon, other factors of interaction should be analysed, such as internal forces in the reinforcement and stresses on the skin of the columns, which goes beyond the scope of this study.

5. Summary and conclusions

The mechanism of transferring loads from the embankment through the geosynthetic-reinforced LTP and columns to the subsoil is complex. It results, among others, from differences in the stiffness of the component materials and complex interactions between them. Despite many studies and extensive experience in the implementation of this type of facilities, failures occur. Low embankments are particularly exposed to uneven settlement. The failure of one of such objects prompted the authors to perform numerical parametric analyses, answering the question of how individual elements of the structural system affect surface deformations.

The complexity of phenomena and the number of influence factors translates into difficulty in modelling this type of objects in geotechnical projects. The second motive to focus on the topic was the answer to the question of how geometrical simplifications of engineering modelling translate into the obtained results.

Based on the analyses carried out, the following conclusions can be drawn:

- The key mechanism for the effective interaction of the GRCSE with the subsoil is the arching phenomenon. The essential design element is the choice of column spacing so that the arching effect occurred in full extend.
- A convenient parameter to characterize the spacing of columns is *ARR*. The increase in *ARR* reduces the settlement itself and the differences in the settlement of surface. The relationship between these parameters is non-linear and after exceeding a certain critical *ARR* value (in the considered structure, this value is about 3.6%) its slight increase causes a significant reduction in deformation.
- Faults at the spacing selection stage are difficult to compensate for with the amount of geosynthetic reinforcement, or the stiffness of the load transmission platform.
- The presence of geosynthetic reinforcement properly pre-tensioned during construction limits the horizontal displacement of the columns.
- In systems with two layers of geosynthetic reinforcement, the bottom layer is of a greater importance.
- The interaction of point-spaced columns with the subsoil is a spatial phenomenon and the most adequate analysis is a 3D simulation. However, due to the availability of software and the time needed to prepare the model and perform the analysis, the simulations under the conditions of a plane deformation or axial symmetry are in common use.
- Settlements and differences in settlements obtained for 2D models using embedded beam elements to represent columns are higher than for 3D models. Similarly, the values of horizontal displacements of the extreme columns are also overestimated.
- It is not a good practice to use only axially symmetric column models in geotechnical designs. It is true that overestimated values of settlements and differential settlements are obtained, which could be treated as conservative design. However, the model does not reflect horizontal deflection due to bending. In the absence of geosynthetic reinforcement, axisymmetric models incorrectly reflect system deformations and thus the methodology should be disqualified as the only tool for analysis.

The above conclusions result from a dozen or so analyses, which, however, concern one engineering object with a specific geometry and mechanical features of the elements, hence caution should be exercised when generalizing them.

References

- [1] M.S.S. Almeida, M. Ehrlich, A.P. Spotti and M.E.S. Marques, “Embankment supported on piles with biaxial geogrids”, *Geotechnical Engineering*, vol. 160, no. 4, pp. 185–192, 2007, doi: [10.1680/geng.2007.160.4.185](https://doi.org/10.1680/geng.2007.160.4.185).
- [2] J. Chu, S. Varaksin, U. Klotz and P. Mengé, “State of the art report: Construction processes”, in *17th Int. Conf. on Soil Mechanics & Geotechnical Engineering: TC17 meeting ground improvement, Alexandria, Egypt, 7.10.2009*, M. Hamza, et al., Eds. IOS Press, 2010, pp. 3006–3135.
- [3] B.R. Christopher, Ch. Schwarz and R. Boudreau, *FHWA NHI-05-037. Geotechnical aspects of pavements*. Washington, D.C., 2006.
- [4] J. Han, “Recent research and development of ground column technologies”, *Ground Improvement*, vol. 168, no. 4, pp. 246–264, 2015, doi: [10.1680/grim.13.00016](https://doi.org/10.1680/grim.13.00016).
- [5] S. Varaksin, B. Hamidi, N. Huybrechts and N. Denies, “Ground improvement vs. pile foundations?”, presented at ISSMGE – ETC 3 International Symposium on Design of Piles in Europe, Leuven, Belgium, 2016, pp. 1–48.

- [6] B. Simon, et al., *Recommendations for the design, construction and control of rigid inclusion ground improvements (Amélioration des sols par inclusions rigides – ASIRI) National Project*. Paris: Presses des Ponts, 2012.
- [7] M.D. Larisch, R. Kelly and T. Muttuvel, “Improvement of soft soil formations by drilled displacement columns”, in *Ground improvement case histories: Embankments with special reference to consolidation and other physical methods*, B. Indraratna, J. Chu, and C. Rujikiatkamjorn, Eds. Oxford: Elsevier, 2015, pp. 573–622.
- [8] B. Simon, “General report S5: Rigid inclusions and stone columns”, presented at ISSMGE – TC 211 Int. Symp. on Ground Improvement IS-GI, Brussels, May 31st & June 1st., 2012.
- [9] A. Krasinski, “Advanced field investigations of screw piles and columns”, *Archives of Civil Engineering*, vol. 57, no. 1, pp. 45–57, 2011, doi: [10.2478/v.10169-011-0005-5](https://doi.org/10.2478/v.10169-011-0005-5).
- [10] J. Han and M.A. Gabr, “Numerical analysis of geosynthetic reinforced and pile-supported earth platforms over soft soil”, *Journal of Geotechnical and Geoenvironmental Engineering*, vol. 128, no. 1, pp. 44–53, 2002, doi: [10.1061/\(ASCE\)1090-0241\(2002\)128:1\(44\)](https://doi.org/10.1061/(ASCE)1090-0241(2002)128:1(44)).
- [11] K. Brzeziński and R.L. Michalowski, “Diffused arching in embankments supported by non-compliant columns with capping beams”, *Computers and Geotechnics*, vol. 132, pp. 1–12, 2021, doi: [10.1016/j.compgeo.2021.104031](https://doi.org/10.1016/j.compgeo.2021.104031).
- [12] Y. Zhuang, S. Hu, X. Song, H. Zhang and W. Chen, “Membrane effect of geogrid reinforcement for Low highway piled embankment under moving vehicle loads”, *Symmetry*, vol. 14, no. 10, 2022, doi: [10.3390/sym14102162](https://doi.org/10.3390/sym14102162).
- [13] R. Rui, J. Han, Y. Ye, C. Chen and Y. Zhai, “Load transfer mechanisms of granular cushion between column foundation and rigid raft”, *International Journal of Geomechanics*, vol. 20, no. 1, 2020, doi: [10.1061/\(ASCE\)GM.1943-5622.0001539](https://doi.org/10.1061/(ASCE)GM.1943-5622.0001539).
- [14] R.P. Chen, Y. W. Wang, X.W. Ye, X.C. Bian and X.P. Dong, “Tensile force of geogrids embedded in pile-supported reinforced embankment: A full-scale experimental study”, *Geotextiles and Geomembranes*, vol. 44, no. 2, pp. 157–169, 2016, doi: [10.1016/j.geotexmem.2015.08.001](https://doi.org/10.1016/j.geotexmem.2015.08.001).
- [15] S.J.M. van Eekelen, A. Bezuijen, H.J. Lodder and A.F. van Tol, “Model experiments on piled embankments. Part I”, *Geotextiles and Geomembranes*, vol. 32, pp. 69–81, 2012, doi: [10.1016/j.geotexmem.2011.11.002](https://doi.org/10.1016/j.geotexmem.2011.11.002).
- [16] P. Shen, C. Xu and J. Han, “Centrifuge tests to investigate global performance of geosynthetic-reinforced pile-supported embankments with side slopes”, *Geotextiles and Geomembranes*, vol. 48, no. 1, pp. 120–127, 2020, doi: [10.1016/j.geotexmem.2019.103527](https://doi.org/10.1016/j.geotexmem.2019.103527).
- [17] L. Brianc¸on and B. Simon, “Performance of pile-supported embankment over soft soil: full-scale experiment”, *Journal of Geotechnical and Geoenvironmental Engineering*, vol. 138, no. 4, pp. 551–561, 2012, doi: [10.1061/\(ASCE\)GT.1943-5606.0000561](https://doi.org/10.1061/(ASCE)GT.1943-5606.0000561).
- [18] D.J. King, A. Bouazza, J.R. Gniel, R.K. Rowe and H.H. Bui, “Load-transfer platform behaviour in embankments supported on semi-rigid columns: implications of the ground reaction curve”, *Canadian Geotechnical Journal*, vol. 54, no. 8, pp. 1158–1175, 2017, doi: [10.1139/cgj-2016-0406](https://doi.org/10.1139/cgj-2016-0406).
- [19] H.L. Liu, C.W.W. Ng and K. Fei, “Performance of geogrid reinforced and pile-supported highway embankment over soft clay: Case study”, *Journal of Geotechnical and Geoenvironmental Engineering*, vol. 133, no. 12, pp. 1483–1493, 2007, doi: [10.1061/\(ASCE\)1090-0241\(2007\)133:12\(1483\)](https://doi.org/10.1061/(ASCE)1090-0241(2007)133:12(1483)).
- [20] B. Ghosh, B. Fatahi, H. Khabbaz, H.H. Nguyen and R. Kelly, “Field study and numerical modelling for a road embankment built on soft soil improved with concrete injected columns and geosynthetics reinforced platform”, *Geotextiles and Geomembranes*, vol. 49, no. 3, pp. 804–824, 2021, doi: [10.1016/j.geotexmem.2020.12.010](https://doi.org/10.1016/j.geotexmem.2020.12.010).
- [21] B. Chevalier, P. Villard and G. Combe, “Investigation of load transfer mechanisms in geotechnical earth structures with thin fill platforms reinforced by rigid inclusions”, *International Journal of Geomechanics*, vol. 11, no. 3, pp. 239–250, 2011, doi: [10.1061/\(ASCE\)GM.1943-5622.0000083](https://doi.org/10.1061/(ASCE)GM.1943-5622.0000083).
- [22] M.T. Suleiman, L. Ni, C. Davis, H. Lin and S.S. Xiao, “Installation effects of Controlled Modulus Column ground improvement piles on surrounding soil”, *Journal of Geotechnical and Geoenvironmental Engineering*, vol. 142, no. 1, pp. 1–10, 2016, doi: [10.1061/\(ASCE\)GT.1943-5606.0001384](https://doi.org/10.1061/(ASCE)GT.1943-5606.0001384).
- [23] H.H. Nguyen, H. Khabbaz and B. Fatahi, “A numerical comparison of installation sequences of plain concrete rigid inclusions”, *Computers and Geotechnics*, vol. 105, pp. 1–26, 2019, doi: [10.1016/j.compgeo.2018.09.001](https://doi.org/10.1016/j.compgeo.2018.09.001).
- [24] J. Wehr, M. Topolnicki and W. Sondermann, “Design risks of ground improvement methods including rigid inclusions”, presented at ISSMGE – TC 211 Int. Symp. on Ground Improvement, Brussels, Paper 35–22E, 2012.
- [25] J. Han, *Principles and practices of ground improvement*. New Jersey: J. Wiley & Sons, Inc., 2015.

- [26] Plaxis 2D Reference manual, Bentley Systems Incorporated, 2019.
- [27] J.J.M. Sluis, F. Besseling and P.H.H. Stuurwold, "Modelling of a pile row in a 2D plane strain FE-analysis", in *Numerical Methods in Geotechnical Engineering*, M.A. Hicks, R.B.J. Brinkgreve and A. Rohe, Eds. London: Taylor & Francis Group, 2014, pp. 277–282.
- [28] T. Lunne, P.K. Robertson and J.J.M. Powell, *Cone penetration testing in geotechnical practice*. London: Blackie Academic, Chapman Hall, 1997.
- [29] S. Marchetti, P. Monaco, G. Totani and M. Calabrese, "The flat dilatometer test (DMT) in soil investigation", A Report by the ISSMGE Committee TC16, in *Proceedings. International Conference on In-Situ Measurement of Soil Properties*. Bali, Indonesia, 2001, pp. 95–132.
- [30] M. Khabbazian, V.N. Kaliakin and C.L. Meehan, "Column supported embankments with geosynthetic encased columns: Validity of the unit cell concept", *Geotechnical and Geological Engineering*, vol. 33, no. 3, pp. 425–442, 2015, doi: [10.1007/s10706-014-9826-8](https://doi.org/10.1007/s10706-014-9826-8).

Analiza deformacji nasypów drogowych posadowionych na kolumnach przemieszczeniowych wzmacniających słabe podłoże gruntowe

Słowa kluczowe: analizy parametryczne MES, kolumny przemieszczeniowe, nasypy drogowe, wzmacnianie podłoża

Streszczenie:

Rozwój infrastruktury komunikacyjnej, ze względu na wymaganą geometrię szlaków, powoduje konieczność wznoszenia obiektów na słabych gruntach. Stosowanie wzmocnień w postaci różnego rodzaju kolumn, które przenoszą obciążenia na głębsze, nośne warstwy gruntu jest w takich sytuacjach powszechne. Wśród tej grupy technologii szczególnie często stosowane są wiercone kolumny przemieszczeniowe, stanowiące wsparcie nasypów.

Pomimo dostępności wielu wyników badań nasypów na kolumnach wzmacnianych geosyntetykami i dużych doświadczeń w ich realizacji, awarie nadal się zdarzają. Motywacją do podjęcia tematu jest przypadek drogi na niskim nasypie, wykonanym na słabym podłożu organicznym wzmocnionym kolumnami (rys. 2) na której wystąpiły duże nierównomierne osiadania nawierzchni. Różnice osiadania stref nad kolumnami i pomiędzy kolumnami miały bardzo różniące się od siebie wartości nawet w sąsiednich polach i wahały się w granicach od 5,5 do 23 mm.

Rozmieszczenie kolumn w planie, pokazano na rys. 3a. Rysunek pokazuje także obszar gruntu przypadający na jedną kolumnę A_s , co pozwala na wyznaczenie tzw. współczynnika wzmocnienia $ARR = A_c/A_s$, gdzie A_c jest polem przekroju poprzecznego kolumny. Na rys. 3b pokazano zastępcze rozmieszczenie kolumn, ułatwiające analizy 2D.

Celem pracy jest zbadanie wrażliwości układu na zmiany wartości istotnych parametrów projektowych, takie jak: geometria i sztywność warstwy transmisyjnej, ilość i sztywność zbrojenia geosyntetycznego oraz rozstaw kolumn, a także na sposób przestrzennego modelowania geometrii konstrukcji. Zadanie wykonano w formie analiz parametrycznych wykorzystując MES. Przedstawiono porównanie wyników uzyskanych dla modeli pojedynczych kolumn w stanie osiowej symetrii (AX), modeli 2D i modeli 3D. Analizując wyniki skupiono się na przemieszczeniach.

Zestawienie analizowanych wariantów modeli przedstawiono w tab. 1. Modele, których parametry są zgodne z parametrami rzeczywistego obiektu nazwano bazowymi i oznaczono dodatkowym symbolem 'b'. Parametry gruntów wykorzystane w modelach numerycznych zamieszczono w tab. 2. Obliczenia wykonano programem Plaxis. Do symulacji warstwy transmisyjnej (ang. LTP) oraz platformy roboczej wykorzystano model Coulomba–Mohra. Do symulacji pozostałych warstw gruntu zastosowano model

Hardening Soil. Obliczenia obejmowały konsolidację gruntu obciążonego w warunkach z drenażem. W analizach 2D i 3D kolumny modelowano z wykorzystaniem elementów 'embedded beams'. Pomędzy warstwy zbrojenia geosyntetycznego i otaczający je grunt wprowadzono warstwę elementów 'interface'.

Rysunek 4 przedstawia porównanie wyników osiadania uzyskanych przy zastosowaniu modelu osiowej symetrii. Wzrost rozstawu kolumn zwiększa osiadania nad głowicami oraz różnice osiadania. Interesujące jest porównanie krzywych odpowiadających modelom AX-b i AX-1, gdzie niewielki wzrost *ARR* spowodował bardzo dużą redukcję osiadania i różnicy osiadania. Zastanawiający jest przebieg krzywej uzyskany przy braku zbrojenia geosyntetycznego. Wyjaśnienia uzyskanych tutaj małych różnic osiadania wymaga jednak dodatkowych analiz.

Rysunki 5 do 8 odnoszą się do rozwiązań uzyskanych w modelach 2D. Rozkład osiadania w modelu bazowym 2D-b przedstawiono na rys. 5. Kolejny rysunek przedstawia porównanie wpływu rozstawu kolumn na osiadania. W tym przypadku, podobnie jak w modelu AX, niewielki wzrost *ARR* (z 3,2% na 3,61%) spowodował znaczne ograniczenia osiadania i różnicy osiadania. Sugeruje to, że istnieje pewna graniczna wartość współczynnika wzmocnienia, powyżej której rozwiązanie konstrukcyjne nabiera pozytywnych cech z punktu widzenia użytkowego.

Wpływ ilości zbrojenia geosyntetycznego, jego rozmieszczenia oraz sztywności, pokazano na rys. 7. Z rys. 7a wynika, że nawet dwukrotny wzrost sztywności zbrojenia nie wpływa jakościowo na redukcję deformacji układu.

Problemy nadmiernych deformacji nasypu, wynikające z dużego rozstawu kolumn, trudno jest także zrekompenzować sztywnością warstwy transmisyjnej, co pokazano na rys. 8.

Rysunek 9 przedstawia zasadnicze elementy modelu 3D oraz uzyskane osiadania nawierzchni.

Na rys. 10 zamieszczono odpowiadające sobie rozwiązania bazowe uzyskane w modelach AX, 2D i 3D. Rysunek ten potwierdza wcześniejsze spostrzeżenia, że w rozwiązaniu osiowosymetrycznym uzyskuje się największe osiadania i największe różnice osiadania, jednakże model ten nie uwzględnia wpływu zginania na wyężenie kolumn.

Próbie wyjaśnienia wpływu rozstawu kolumn na deformacje nasypu przedstawia rys. 11. Pokazano na nim trajektorie naprężeń głównych uzyskane w rozwiązaniach 2D-b (*ARR* = 3,2%) oraz 2D-s4 (*ARR* = 4,18%). W pierwszym przypadku, duży rozstaw kolumn, przy ograniczonej wysokości nasypu uniemożliwił pełne rozwinięcie się efektu przesklepienia.

Na rys. 12 zestawiono wszystkie poprzednio omówione rozwiązania, wyliczając dla każdego z nich efektywność transferu obciążenia na kolumnę, zdefiniowaną formułą (4.1) w funkcji różnicy osiadania.

Z przeprowadzonych symulacji wynika, że sposób modelowania geometrii (AX, 2D i 3D) jest istotnym czynnikiem wpływającym na uzyskane wyniki opisujące deformacje nasypu. W niskich nasypach bardzo istotnym parametrem projektowym jest rozstaw kolumn i związany z nim współczynnik wzmocnienia *ARR*. Zbyt mała wartość tego współczynnika uniemożliwia pełne rozwinięcie się efektu przesklepienia, redukując efektywność rozwiązania i prowadząc do dużych wartości osiadania i różnic osiadania. Błędy na tym etapie projektowania trudno jest zrekompenzować przez ilość i sztywność zbrojenia geosyntetycznego, czy też zagęszczenie (sztywność) warstwy transmisyjnej. W rozważanym przypadku krytyczna wartość parametru *ARR*, powyżej której deformacje układu ulegają znacznej redukcji wynosi około 3,6%.

Przeprowadzone analizy dotyczą tylko jednego nasypu i należy zachować ostrożność przy próbie uogólniania przedstawionych wniosków.